

M. Eigenfeld, R. Kerpes, J. Bez and T. Becker

Upcycling of brewer's yeast – Application as material for encapsulating unstable liquid ingredients in the food industry

Encapsulation refers to the process of equipping an active compound with a relevant wall material in order to protect it. Owing to the flexible protein structure combined with rigid polysaccharide content, yeast cell walls are considered ideal for encapsulation. Additionally, the low price and availability are further advantages that render yeast cells a suitable material for encapsulation. However, since yeast cells used in the brewing process retain a bitter taste from the adsorption of iso- α acids, it is essential to upcycle spent brewer's yeast prior to its possible application as an encapsulation material. The upcycling process presented here was carried out in three main stages: (i) debittering, (ii) fragmentation of spent brewer's yeast and (iii) encapsulation by using yeast cell wall fragments. A maximum removal of bitterness of 78.08 % was identified at 6 °C, pH 9 and after 30 min of debittering. The average residual bitterness was 0.51 ± 0.12 mg Iso- α -L-g wet weight. Three subsequent sessions of high-pressure homogenization at 800 bar were appropriate to achieve maximum cell disruption of more than 90 % and a $D_{0.5}$ value of 0.0875 μm . A high encapsulation efficiency, determined in encapsulation trials with seed oil, indicated that yeast cell walls are suitable as material for encapsulating fatty acids and can replace or even exceed the gum arabic reference system. Encapsulation of more than 90 % of the initial amount of oil were possible. The results obtained from the experiment suggest that the employment of high-pressure homogenisation at optimal temperature and pressure achieved maximum encapsulation efficiency and that yeast cell wall fragments can be considered as an appropriate substitute for gum arabic.

Descriptors: encapsulation, yeast, spent brewer's yeast, upcycling, bitter compounds

1 Introduction

Over the past few years, a growing number of foods that are enriched with functional ingredients have become established on the market. Owing to the influence of external factors such as oxygen and UV light, these ingredients quickly lose their original functionality. However, volatile and unstable components can be protected by microencapsulation. Encapsulation refers to the process of coating an active compound, called a core material, with a relevant wall material, named a shell. This process is carried out to keep the flavour of a food product stable or to prevent it from losing its characteristics due to environmental changes, such as evaporation, oxidation or chemical reactions [1]. It is an effective commercial process that is primarily used in the food and beverage industry and employs several methods, such as freeze-drying, spray-drying-coupled chilling and molecular inclusion [2]. The type of

encapsulation technique mainly depends on the conditions applied during production and on its end usage. Commercially, the most common encapsulation material (for spray drying applications) is gum arabic, which is considered expensive and subject to price fluctuations. Therefore, spent brewer's yeast is expected to be a suitable and affordable alternative that can regain organic residues from food products. Moreover, it is permanently available as a by-product of the brewing process [3, 4]. On a global scale, over 400,000 tonnes of spent brewer's yeast are generated during the brewing process each year. Owing to the high content of protein, ranging from 45 % to 60 %, various minerals and B complex vitamins, spent brewer's yeast is primarily fed to monogastric animals [5, 6]. Therefore, little benefit is often gained from it and it is considered an innately inferior source. However, it can be effectively upcycled to yield a high-quality raw material that improves the benefits for yeast recyclers and breweries at the same time [6–8]. Additionally, yeast cells have a generally recognised as safe (GRAS) status, so they can be used without problems for food and food ingredients [9].

The yeast cell wall occupies approximately 15–30 % of the dry yeast cell space and is considered a suitable encapsulation material due to (I) its chemical composition, (II) the simultaneous presence of proteins and polysaccharides, (III) its sufficient stability and (IV) the targeted release of encapsulated substances [10]. In most applications, a combination of carbohydrates and proteins is used as this combination is not only stable, but also offers excellent encapsulation efficiency compared with other materials [11]. The

<https://doi.org/10.23763/BrSc20-10eigenfeld>

Authors

Marco Eigenfeld, Roland Kerpes, Thomas Becker, Technical University of Munich, Chair of Brewing and Beverage Technology, Research Group Beverage and Cereal Biotechnology, Freising, Germany; Jürgen Bez, Fraunhofer Institute for Process Engineering and Packaging IVV, Freising, Germany; corresponding author: roland.kerpes@tum.de

cell wall structure of *S. cerevisiae* is resilient yet elastic owing to the presence of large quantities of mannoproteins, chitin and rigid β -glucan [12]. The mannoprotein layer on the surface of the yeast cell filters molecular particles. β -glucan is responsible for the morphological shape and stability of the cell wall, while chitin components are responsible for rigidity, strength and protection of the cell interior [13–20]. Next to protecting the cell from external influences, the cell wall structure of *S. cerevisiae* yeast cells is in charge of controlling mass transfer and osmotic pressure. In addition, as yeast cell walls originate from non-animal sources, they are suitable for vegan consumers [6, 21–23].

All of these factors render the yeast cell wall an appropriate encapsulation material; however, brewer's yeast contains a pungent bitter taste that is counterproductive to the very purpose of its use as an encapsulation material. Additionally the use of whole yeast cells as encapsulation material make limitations according to the capsule size, which is limited to the initial cell size. Besides the linseed oil encapsulation presented in this paper, essential oils have already been successfully encapsulated in whole *S. cerevisiae* cells by using passive diffusion [24]. Some of the advantages reported included that the oil profiles remained intact due to the cell structure as well as the protective effect exerted by the cell membrane. Furthermore, probiotics such as specific *Lactobacillus* strains have already been successfully encapsulated by using yeast cell walls. Some of the advantages reported for this application were improved metabolic activity and the increased survival of probiotics in the encapsulation shell [7, 25]. Capsules containing valuable ingredients such as flavourings or fatty acids that are used in the beverage industry were also generated by using empty yeast cells as a delivery system. Encapsulation efficiency of $\geq 50\%$ (encapsulated oil related to the initial amount of oil) for flavour compounds and the fact that water is needed to initiate release are designated as favourable properties of this system [26]. Owing to the listed advantages of a stable cell wall structure, the low price and the very good availability of yeast cells, we present in this paper a process for upcycling spent brewer's yeast and a subsequent encapsulation procedure to produce yeast cell wall capsules for applications in the food and beverage industry. Due to the use of high-pressure homogenization as the method of choice for cell fragmentation, the resulting encapsulation process is not limited to initial yeast cell sizes and therefore more flexible according to the resulting capsule size.

2 Materials and Methods

The process of upcycling bottom-fermenting spent brewer's yeast to the final product of capsules included five steps: debittering, microscopic evaluation, fragmentation, characterisation and encapsulation.

2.1 Debittering

Debittering of bottom-fermenting spent brewer's yeast was carried out by separating the cell pellet and the supernatant (5 min, 4000 rpm). The pellet was washed three times with potassium phosphate buffer (50 mM, pH 6.5) in 50 mL reaction tubes. The cell pellets were resuspended in potassium phosphate buffer solution. pH

adjustment was carried out by adding sodium hydroxide solution followed by different incubation periods at specific temperatures on an overhead shaker. The debittering process was optimised by varying three parameters, namely, pH (8.0 or 9.0), debittering temperature (0 or 6 °C) and debittering duration (10 or 30 min), using a fully factorial experimental design, resulting in eight different experiments performed in triplicate.

2.2 Determination of bitter compounds

HPLC analysis was conducted to quantify the iso- α -acid content in the supernatant according to the MEBAK method 4.3.3.1 [27]. International Calibration Extract (ICE) and dicyclohexylamine (DCHA) standards were included. The detection of iso- α -acids was carried out with a UV / Vis detector at 270 nm, while that for α -acids was at 314 nm.

2.3 Modified MEBAK method

In addition to the HPLC analysis to exclusively determine the bitter compounds in the supernatant of separated yeast cells, a modified MEBAK method (MEBAK 2.18.1) [28] was used to determine the content of bitter substances that are bound to the yeast cell wall. For the quantification of bitter compounds on the yeast cell wall, cropped yeast of the second, third, sixth and seventh pitches, as well as spent brewer's yeast after the seventh pitch, was used.

Yeast pellets weighing 0.1 – 0.5 g were completely dissolved in 10 mL of de-ionised water in 50 mL flasks. A total of 0.2 mL of hydrochloric acid (HCl) (25 %) and 2 mL of isooctane were added and the suspension was stirred at 400 rpm for 20 min. To ensure phase separation, subsequent centrifugation was carried out at 3,000 rpm for 4 min. The upper organic phase was removed and transferred to a quartz cuvette. The photometric measurement was executed at 275 nm against isooctane in a quartz glass cuvette. The calculation of the bitterness, expressed as the iso- α -acid content in mg/L, was determined after calibration using different concentrations of a dicyclohexylamine standard. The regression curve was calculated as $y = 0.1496x$ with an R^2 of 0.996.

2.4 Microscopic evaluation

Microscopic evaluation was performed to find out whether yeast cell contamination with bitter substances could be qualitatively determined. For this evaluation via scanning electron microscopy (SEM), samples needed to be vacuum-stable, which implies that no water evaporates and interferes with the flow of electrons during analysis. By using SEM, fresh bottom-fermenting yeast samples, cropped yeast from the third pitch and spent brewer's yeast after the seventh pitch were evaluated. One cell pellet of each yeast sample was washed in PBS buffer and fixed for 1 h by gentle shaking with glutaraldehyde (2.5 %) at room temperature. Using PBS buffer, the suspension was washed again and the pellet was resuspended. After an incubation period of 10 min on a glass slide, the slide was dehydrated by a series of ethanol solutions with increasing concentrations up to a final concentration of 100 % EtOH. This last step was repeated three times with 100 % EtOH and the glass slides were dried in a desiccator. Furthermore, the yeast slides were sputter-coated with gold particles to increase

conductivity and contrast. The prepared yeast cells were examined in a JSM-5900 LV scanning electron microscope (JEOL, Tokyo, Japan) using a voltage of 15 kV and a magnification of 10,000. Further settings entailed an accelerating voltage of 15, a spot size of 20, SEI signal setting, a WD of 47 in case of fresh yeast, and a WD of 46 for cropped and spent brewer's yeast.

2.5 Transfer to yeast from higher pitches

To verify the reproducibility of the debittering method and the bitter compound quantification methods, various pitches of bottom-fermenting, cropped and spent brewer's yeast were processed with regard to the efficiency of the debittering process scheme. For this purpose, cropped yeast from the second, third, sixth and seventh pitches was debittered using the optimised method and the bitterness content before and after debittering was determined by the modified MEBAK method.

2.6 Fragmentation

For several years, researchers used high-pressure homogenisation (HPH) for the fragmentation of brewer's yeast cells. To understand which parameter settings were optimal for encapsulation with cell wall fragments, different pressures between 300 and 1,000 bar were applied in one to five intervals using an APV 1000 (APV Systems, Albertslund, Denmark) system. Additionally, single and two-step homogenisation was applied, as well as optimal inlet temperature and dry matter content of the suspended yeast cells.

After the homogenisation process, the yeast cells were microscopically examined to quantitatively determine the level of cell disruption using a counting chamber. For this analysis, the centrifuged yeast pellet was diluted with PBS at a ratio of 1:20. To determine the viability of yeast before and after HPH, aliquots of 100 µL of the diluted yeast samples were stained with 10 µL of methylene blue. The number of dyed cells in relation to the total number of cells indicated the percentage of dead cells. The degree of disruption was calculated by relating the number of intact (viable) cells after HPH to the total number of viable cells of the untreated yeast sample.

2.7 Structural characterisation

In the next step, the yeast cells were subjected to structural characterisation by measuring the particle sizes via static light using a Mastersizer3000 (static light scattering, wet dispersion unit; Malvern Paralytical GmbH, Kassel). The suspensions were analysed for the yeast cell particle sizes before (Y0) and after debittering as well as before (Y1) and after fragmentation (Y2). Furthermore, calculations were carried out with regard to a refractive index of 1.4 and an absorption coefficient of 0.001. The dispersion medium was water with a refractive index of 1.33 and it was blanked for 10 s with blue and 10 s with red light. Samples were dispersed in the water to shading of 5 %. Measurements were started after a 30 s delay for stabilisation of the dispersion. All samples were measured five times with a delay of 30 s. Digested (=subjected to HPH) samples were subsequently compared with native samples, which served as a reference. It is important to emphasise the difference between the numeric and volume distributions of particles. The volume distribution is required for material processes due to

the importance of the particle volume for system properties and composition and places a higher weighting on large particle sizes. In contrast, the numeric distribution is required for monitoring the efficiency of the fragmentation process due to the higher weighting of small particle sizes.

2.8 Encapsulation

In the encapsulation step, the primary target was the development of methods that were capable of defining emulsion stability and efficiency of the encapsulation technique. To determine to what extent encapsulation is feasible for yeast cell fragments, the amount of gum arabic (GA) in the emulsions was substituted with yeast cell fragments, while the amounts of oil and maltodextrins (MD) were kept constant. Emulsions with 15 % dry matter, 9 % (related to dry matter) oil content and a constant ratio of MD vs. GA or yeast fragments of 1:1 were prepared. GA was substituted in 20% steps with yeast cell fragments up to complete substitution. Simultaneously, the percentage of oil was increased in three steps up to 25 %. Moreover, various parameters of the yeast cell emulsions such as pH, particle size (static light scattering; Mastersizer3000), viscosity (Rheometer AntonPaar MCR301) and stability (TurbiScan Lab) were recorded to assess the efficiency of encapsulation.

The capsules were produced by spray-drying the emulsions (Büchi Labortechnik, Essen, Germany) with an air inlet temperature of 180 °C and air outlet temperature of 80–85 °C. For each sample, approximately 800 mL of emulsion was fed and the pump feed rate was continuously adjusted in order to guarantee an air outlet temperature in the range of 80 °C to 85 °C.

2.9 Encapsulation efficiency

Finally, the capsules were spray-dried and the proportion of surface oil was determined to evaluate the efficiency of the encapsulation technique. The encapsulation efficiency is expressed as the percentage of oil incorporated in the capsules related to the initial amount of oil. Determination of the encapsulation efficiency was adapted from the work of *Carneiro* et al., who examined the oxidative stability and encapsulation efficiency of flax seed oil using spray-drying [29]. To analyse the non-encapsulated (surface) oil, a fixed amount (~ 1.5 g) of dry capsules were weighed into volumetric flasks, defined amounts of n-hexane were added and the flasks were shaken by hand for 2 min. The solvent mixtures were then filtered through Whatman filters No. 1 (pore size: 11 µm) and the remaining powders on the filters were rinsed three times with 20 mL of hexane. The solvents were collected in pre-dried (105 °C, overnight) glass jars and left to evaporate at room temperature to a constant weight. The mass differences between the jars containing the extracted oil residues and the tare weights of the jars corresponded to the masses of non-encapsulated oil. In accordance with the literature method, it was assumed that the initial oil was completely encapsulated and was equal to the total oil. The encapsulation efficiency was calculated from the amounts of surface oil and total oil as follows [29]:

$$\text{Encapsulation efficiency [\%]} = \frac{\text{Total oil}_{\text{recipe}} \left[\frac{\text{g}}{100 \text{ g}} \right] - \text{Surface oil} \left[\frac{\text{g}}{100 \text{ g}} \right]}{\text{Total oil}_{\text{recipe}} \left[\frac{\text{g}}{100 \text{ g}} \right]} \cdot 100$$

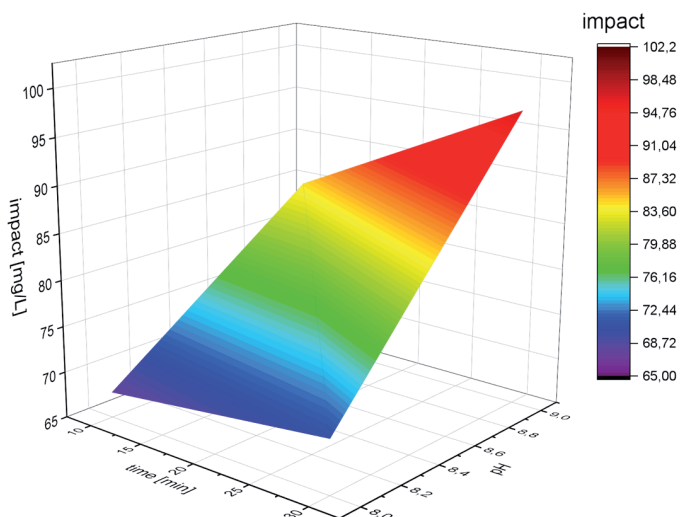


Fig. 1 Content of iso- α acids in the supernatant after the first debittering step at different pH values and exposure times. Tested range: pH 8.0 – 9.0, time: 10 – 30 min; N = 3

3. Results and discussion

3.1 Upcycling of spent brewer’s yeast

Since the debittering of yeast requires a gentle and extensive process, yeast cells were carefully washed in three steps and the debittering was conducted in two steps. According to the full factorial model, various settings of parameters including temperature, pH and exposure time were compared in interaction with each other with regard to achieving the greatest possible debittering rate, measured in the supernatant of centrifuged yeast samples. Measurements were performed in accordance with the HPLC analysis described in 2.2. As shown in figure 1, the results of debittering effects showed significant differences between pH and debittering time. In general, all experiments using a higher pH showed a higher content of bitter compounds in the supernatant of around 21.5 mg/L after the first step of debittering. The increase of debittering duration had a positive impact. For example, an additional 20 min of exposure time in the debittering environment resulted in an increase of bitter compounds in the supernatant from 86.6 ± 9.9 mg/L to 102.2 mg/L ± 2.6 . The variation of temperature had a lower impact on debittering and thus is not shown in the diagram.

To express these results in a statistical way, all eight experimental situations (see section 2.1) can be evaluated using ANOVA. The impact of the debittering effect was highly influenced by pH (F-test p-value < 0.0001). Additionally, the variation of exposure time had a significant impact on debittering efficacy, verified by an F-test (p-value 0.0044). This indicated that 99.56 % of the fully factorial model would be modulated by this parameter. The interaction of the two factors, pH value and exposure time, was calculated to an F-test p-value of 0.0290. R^2 of the model (calculated from 23 of the 24 tested points) was determined as 0.82. According to these results, a maximum yeast cell debittering rate in the tested range was achieved at 6 °C, pH 9 and a debittering period of 30 min. In several studies on this subject, almost complete removal of bitterness with regard to the sensory perception of it was achieved

[21, 22]. The debittering of the yeast cells at pH 10 or 11 and temperatures of 45 °C to 50 °C had been a common and efficient method [21, 22], but the debittering process at lower pH values and temperatures resulted in a higher debittering rate, yeast viability and process cost-effectiveness. Additionally a denaturing effect of mannoproteins can be avoided because of the use of lower temperatures and gentle pH-values. Subsequent to the debittering, microscopic evaluation and measurements of non-debittered and debittered samples were performed to qualitatively evaluate and quantitatively analyse the effects of this process.

3.2 Quantitative analysis and qualitative microscopic evaluation of brewer’s spent yeast

The contamination of yeast cells by adsorbed bitter compounds was quantitatively analysed to determine the impact of debittering and residual bitterness. In contrast to the process described in the previous chapter, the quantification is performed by the modified MEBAK method, described in section 2.3.

One of the major issues in this context was that established quantitative methods such as HPLC analysis only focus on bitter compounds in solution. By applying a modified MEBAK method [28], it was possible to photometrically quantify the bitter compounds that were bound to the yeast cells.

The results obtained from cropped bottom-fermenting yeast cells showed an average debittering rate of 77.6 %, expressed as mg iso- α -L-g dry weight (Fig. 2). The spent brewer’s yeast resulted in the loss of 78.08 % iso- α -acids. The average residual bitterness of all samples was determined as 0.51 ± 0.12 mg iso- α / L-g wet weight.

During the examination of yeast via SEM, certain morphological deformations of the cell surface (indentations) were observed with increasing re-pitch rates. However, those changes were primarily

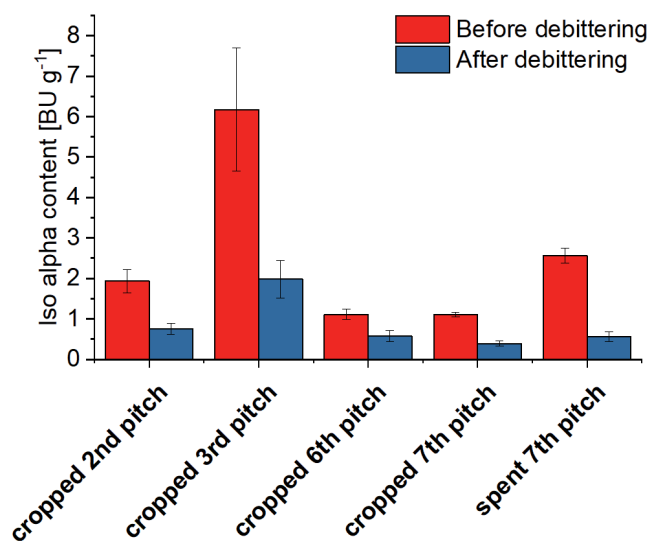


Fig. 2 Comparative measurement of the bitter substances bound to the yeast cell wall before and after the debittering at a pH of 9, a temperature of 6 °C and a debittering time of 30 min; N = 3

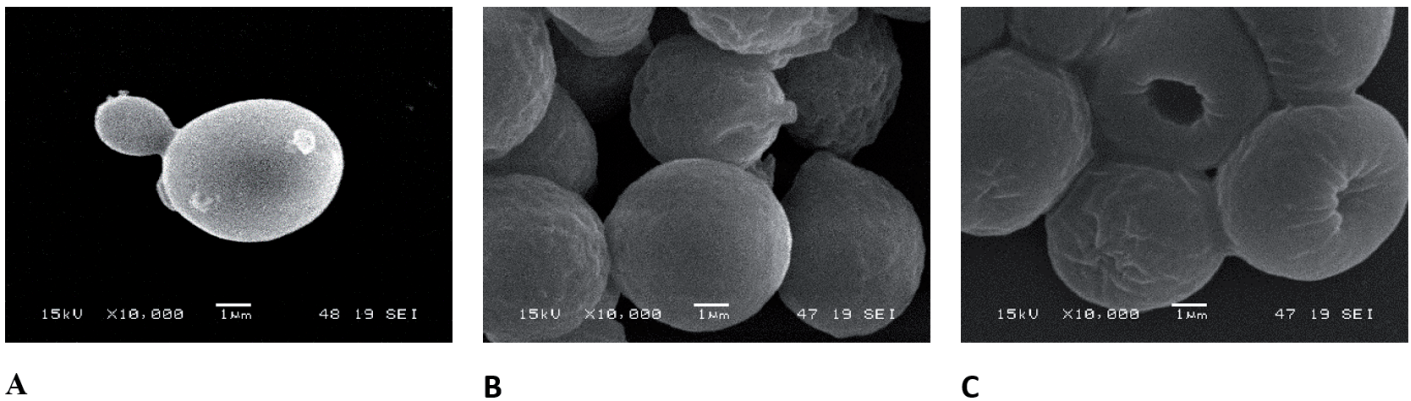


Fig. 3 Fresh bottom-fermenting yeast (A), cropped yeast from the third pitch (B) and spent brewer's yeast after the seventh pitch (C)

evident in cropped yeast (Fig. 3 C) rather than in fresh yeast (Fig. 3 A). Pitched yeast seemed to have a rougher surface with wrinkles (Fig. 3 B). The spent brewer's yeast in particular had an atypical morphology (Fig. 3 C).

This change in morphological change occurs due to osmotic pressure by the medium, namely, ethanol and high sugar concentrations. Pratt et al. [30] were able to show similar effects of osmotic pressure and ethanol concentrations on the yeast morphology, resulting in a shrinkage of the cells, a change in yeast cell wall surface and in the appearance of indentations. The effects of salt and sugar osmotic stresses were also determined by Avila et al. [31] and found to result in similar morphological changes. A correlation between the morphology of yeast cells and the absorbed bitter compounds could not be examined by SEM. However, after the debittering process, changes in the cell wall surface or morphology were visible (Fig. 4). It could be seen that debittered bottom-fermenting yeast cells seemed to be less aggregated and could be found preferably at the single-cell stage (Fig. 4 B and D). In comparison to these observations, non-debittered cells (Fig. 4 A and C) had a strong tendency to form cell aggregates with multiple cells. Additionally, the surface of debittered yeast cells was free of contaminations in comparison to non-debittered cells (Fig. 4 C), which shows, that yeast cells form aggregates due to the Iso- α acids, which are bound to the cell wall surface.

3.3 Fragmentation

HPH was optimised to avoid increased temperatures $> 40^{\circ}\text{C}$ in order to prevent autolysis of the cells. Another objective was the achievement of the highest possible degree of yeast cell disintegration.

The disruption of yeast cells occurred more rapidly with increasing homogeniser pressure (Fig. 5). Similarly, at all pressures, there was a significant increase in digestion level with an increasing number of runs; however, the pressure-dependent increases were non-linear with no specific pattern. No complete

cell disruption was achieved by the application of 300 and 400 bar (93 and 96 %, respectively, after five runs). Upon pressurisation of 600 bar or higher, a sufficient level of disruption ($\geq 97\%$) was already achieved in two runs. The highest pressure of 800 bar resulted in a percentage disruption of 98 %. Five runs at pressures ≥ 600 bar were necessary for complete digestion (99 – 100 %). However, pressurisation of 800 bar resulted in a sample temperature of 41°C after five runs, which is above the temperature limit of 40°C .

A two-step homogenisation process did not improve the digestion levels of the one-step process. Similarly, the dry matter (DM) content did not influence the degree of digestion; however, lower DM values resulted in longer processing intervals.

On the other hand, HPH with 600 and 800 bar and 1 – 5 runs resulted in significant differences between fresh and cropped bottom-fermenting yeast samples. Pressure of 800 bar was determined

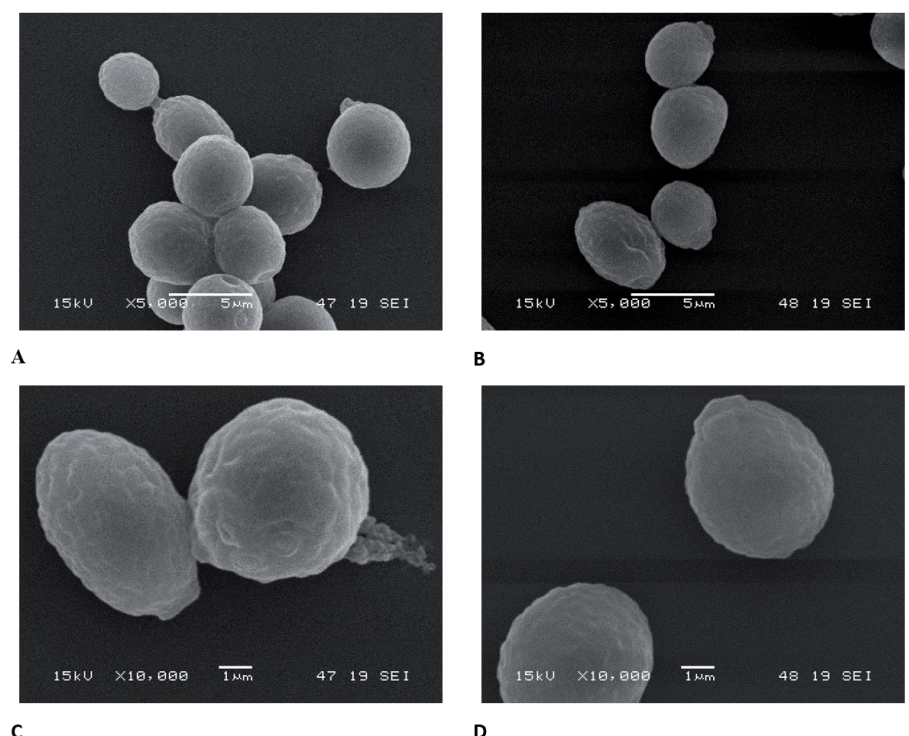


Fig. 4 Cropped bottom-fermenting yeast from the third pitch before debittering (A and C), and after debittering (B and D). A and B: 5,000 times magnification; C and D: 10,000 times magnification

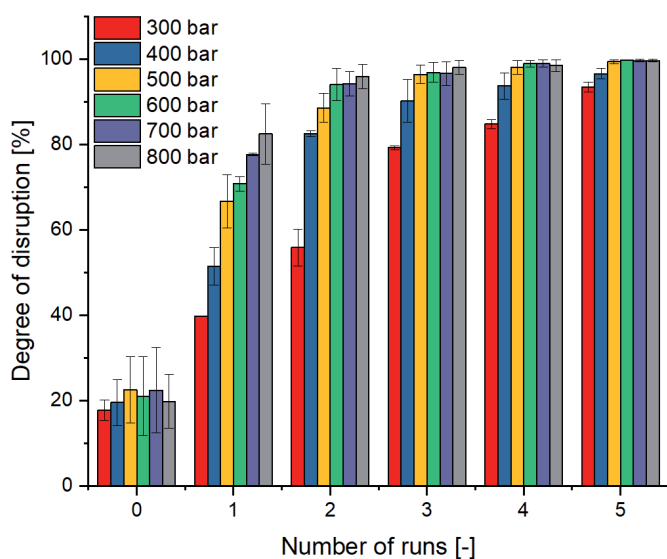


Fig. 5 High-pressure homogenisation of cropped yeast; percentage degree of digestion depending on pressure and number of runs; average values of two test series

as the minimum requirement for complete digestion ($\geq 98\%$) of fresh yeast samples. The results illustrated that HPH is one of the most efficient techniques for achieving maximum cell disruption at reproducible rates by selecting suitable settings.

3.4 Structural characterisation

The yeast cell characterisation based on the particle size distribution of fresh yeast and non-debittered disrupted spent brewer’s yeast resulted in significant deviations. Determination of the particle size distribution of yeast cell fragments is important to predict the quality of the encapsulation process. In general, fresh bottom-fermenting yeast cells show only one peak (6 – 8 μm) due to the homogeneous spherical shape; peaks at greater values indicate cell agglomerations. To evaluate the data, the particle size distributions of fresh yeast (Y0), debittered, undisrupted yeast suspension (Y1) and non-debittered, digested spent brewer’s yeast (Y2) were compared.

The comparison of volume distributions (D_3) of cells is performed using the characteristic $D_3(50)$ value of a sample, describing the volumetric diameter of 50% of the measured particles. The second value that was determined per sample is the numeric distribution $D_0(50)$.

The $D_3(50)$ value of the debittered yeast Y1 was determined as 6.92 μm , which is significantly smaller than the value of the fresh yeast Y0 determined as 13.45 μm . In contrast, the volume diameter of the disrupted yeast cells Y2 was determined as 4.39 μm with a $D_0(50)$ value of 0.0875 μm , indicating a wide particle size distribution. In comparison, the $D_0(50)$ of the fresh yeast sample Y0 of 8.08 μm implied a significantly higher number of large

particles. The particle size needed for encapsulation depends on the method used for the encapsulation [32]. Owing to the following application of spray drying, a particle size in the range of 1 – 50 μm is favourable [33]. A low surface-to-volume ratio of the particles is necessary for high encapsulation efficiency [34]. Therefore, larger capsules with a wide particle size distribution are favourable for low porosity and a high surface-to-volume ratio.

3.5 Encapsulation

For encapsulation experiments, emulsions with a constant linseed oil content of 9% and varying ratios of GA and yeast cell wall fragments (CWF) were mixed. The gradual substitution of GA by CWF resulted in increasing particle sizes ($=D_0(50)$ values) of the respective emulsions, ranging from 0.6 μm for the reference system to 5.6 μm for the 100% substituted capsules. This range for microcapsules is smaller than the one described in the literature [7, 35]. Depending on the application of spray drying, a particle size of the powder in the range of 1 – 100 μm is conceivable [33, 37]. *Tonon* et al. measured a similar diameter range for spray-dried powders of flaxseed oil in GA shells of $D_0(50) = 9.15 - 17.88 \mu\text{m}$, depending on the drying conditions [38]. Thus, the results obtained are comparable to those particle sizes [37, 38].

Upon evaluation of emulsion stability, expressed by the Turbiscan Stability Index (TSI), a correlation between the content of GA and stability was not observed. Via TSI, which characterises the sum of all destabilisation processes such as sedimentation [39], the emulsion stability was evaluated. The stability after 8 h (TSI global, $t = 29^\circ\text{C}$, isotherm) was the smallest for the reference system with 100% GA (TSI 0.8). For the emulsion with varying amounts of CWF components, the TSI values ranged between 0.9 and 1.2. In general, a lower TSI value indicates increasing stability of the emulsion and a reduced probability of phase separation due to sedimentation, flotation or agglomeration [40]. The measured

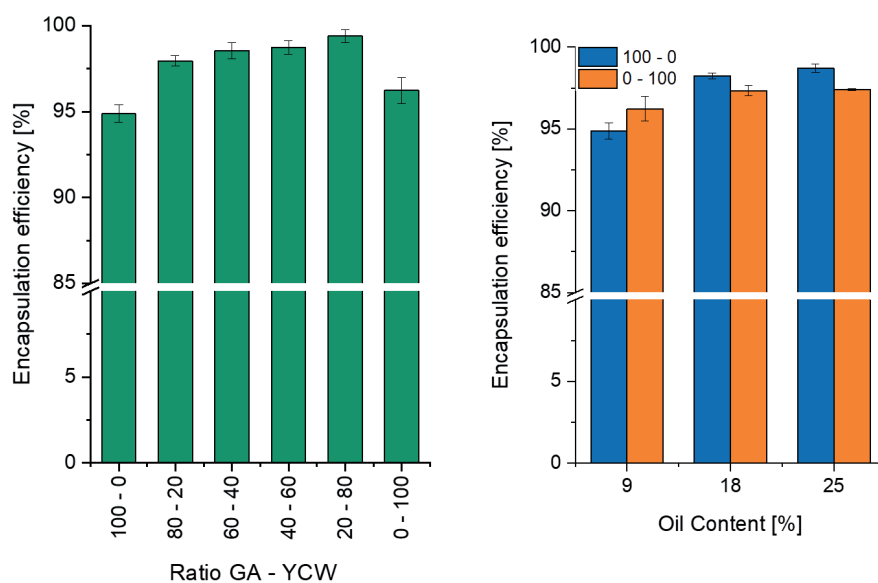


Fig. 6 Left: Encapsulation efficiencies of systems with varying proportions of GA and CWF with a constant oil content of 9%. Right: Encapsulation efficiencies of the 100% GA (100 – 0, blue bars) and the 100% CWF systems (0 – 100, orange bars) with varying oil proportions

values indicate destabilisation at a very early stage without any visual observation.

The encapsulation efficiencies, expressing the percentage of incorporated oil compared with the initial oil, for the different GA/CWF ratios and the 100 % CWF system were higher than that of the reference system (100 % GA). The highest encapsulation efficiency was determined as 97.4 % for the 20% GA/80 % CWF system (Fig. 6 left). Variations of the initial oil contents in 100 % GA capsules resulted in additional differences in encapsulation efficiency (see Fig. 6, right). The encapsulation efficiency of the 100 % GA capsules, designated as the reference system, increased from 94.8 % (9 % oil) to 98.7 % (25.4 % oil). The 100 % CWF system encapsulation efficiency was less affected by varying oil contents, displaying only small ranges between 96 and 97 %. With increasing oil content, the reference system efficiency exceeded the one of the challenging system. For a used ratio of oil:yeast cells < 0.25, efficiencies greater 90 % were reported. Salari et al. [41] determined an encapsulation efficiency of 78 ± 0.6 % for berberine, encapsulated in freeze-dried yeast cells. Another study also resulted in comparable values for the encapsulation efficiency of around 98 %, depending on the ratio of core to wall material [42].

4 Conclusion/Summary

This study was intended to establish suitable procedures for the purification and debittering of spent brewer's yeast as well as for the complete HPH disruption of yeast cells for cell wall fragmentation. It was shown that a bitterness loss of 78.08 % was achievable by using an optimised and gentle debittering method. Comparing this process to literature, denaturation effects due to high temperature is minimized as well as reduced traces of chemicals. The average residual bitterness of all samples was determined to be 0.51 ± 0.12 mg iso- α -L-g wet yeast weight, which is considered an acceptable value. Yeast CWF obtained from spent brewer's yeast by cell disruption are a suitable material for encapsulating unstable liquid ingredients such as unsaturated fatty acids as shown by increased encapsulation efficiency of 97.4 % compared with the industrially used encapsulation raw material GA with an efficiency of 94.8 %. The described procedures can be established in breweries or yeast extract manufacturers by upcycling a by-product such as spent brewer's yeast. Advantages of the method on hands are the possibility of the capsule packaging due to the loss of size limitations. The cell wall fragmentation by HPH allows the production of capsules of sizes below 6 μ m, so these are less detectable in food products. Additionally, a faster target release could be performed, because the release mechanism is not diffusion controlled. The oil release in whole yeast cells is totally diffusion controlled and takes more time than a disintegration of packed capsules. Therefore, the method on hands is a more flexible system compared to established yeast encapsulation processes. Due to the reduced size of capsules, a drying process and implementation into food and beverages a less sedimentation is conceivable. Comparable to capsules described in the literature, that were produced by incorporation of oil into whole yeast microcapsules, a coating of the presented capsules can also be performed to protect encapsulated oil against oxidation. In conclusion, this new and innovative product enables the development of further market segments for

spent brewer's yeast and a possible decrease of encapsulation costs due to cheaper raw materials while the protection of unstable ingredients is enhanced. Moreover, this method can be implemented due to the flexibility of capsule size.

Acknowledgement

This research project was supported by the German Ministry of Economics and Technology (via AiF) and the IVLV (Industrievereinigung für Lebensmitteltechnologie und Verpackung e.V), Project AiF 19196N. The authors would furthermore like to thank Dr Michael Quantz (VH Berlin, Berlin) for supporting the project and Michael Schott for discussions about structural characterisation and encapsulation. Additionally, we thank Dr Thomas Heidebach (ADM Wild Europe GmbH & Co. KG) for discussions of applications and providing raw materials for encapsulation experiments and Dr Markus Blaesen (Leiber GmbH) for support with yeast shells as raw material and the method for bitter compound determination.

5 References

1. Vasisht, N.: Chapter 16 – Selection of Materials for Microencapsulation, in *Microencapsulation in the Food Industry*, A.G. Gaonkar, et al., Editors. 2014, Academic Press: San Diego. p. 173-180.
2. Đorđević, V.; et al.: Trends in Encapsulation Technologies for Delivery of Food Bioactive Compounds. *Food Engineering Reviews*, 2014.
3. Paramera, E.I.; Karathanos, V.T. and Konteles, S.J.: Chapter 23 – Yeast Cells and Yeast-Based Materials for Microencapsulation, in *Microencapsulation in the Food Industry*, A.G. Gaonkar, et al., Editors. 2014, Academic Press: San Diego. p. 267-281.
4. Meng, Y. and Cloutier, S.: Chapter 20 – Gelatin and Other Proteins for Microencapsulation, in *Microencapsulation in the Food Industry*, A.G. Gaonkar, et al., Editors. 2014, Academic Press: San Diego. p. 227-239.
5. Chae, H.J.; Joo, H. and In, M.-J.: Utilization of brewer's yeast cells for the production of food-grade yeast extract, Part 1: effects of different enzymatic treatments on solid and protein recovery and flavor characteristics, *Bioresource Technology*, **76** (2001), no. 3, pp. 253-258.
6. Pérez-Torrado, R.; et al.: Yeast biomass, an optimised product with myriad applications in the food industry, *Trends in Food Science & Technology*, **46** (2015), no. 2, Part A, pp. 167-175.
7. Mokhtari, S.; et al.: The cell wall compound of *Saccharomyces cerevisiae* as a novel wall material for encapsulation of probiotics, *Food Research International*, **96** (2017), pp. 19-26.
8. Shotipruk, A.; et al.: Application of rotary microfiltration in debittering process of spent brewer's yeast, *Bioresource Technology*, **96** (2005), no. 17, pp. 1851-1859.
9. Nakhaee Moghadam, M.; Khameneh, B. and Fazly Bazzaz, B.S.: *Saccharomyces cerevisiae* as an Efficient Carrier for Delivery of Bioactives: a Review, *Food Biophysics*, **14** (2019), no. 3, pp. 346-353.
10. Aguilar-Uscanga, B. and François, J.M.: A study of the yeast cell wall composition and structure in response to growth conditions and mode of cultivation, *Letters in Applied Microbiology*, **37** (2003), no.3, pp. 268-274.
11. Gibbs, F.; et al.: Encapsulation in the food industry: a review, *International Journal of Food Sciences and Nutrition*, **50** (1999), no. 3, pp. 213-224.
12. Orlean, P.: Architecture and biosynthesis of the *Saccharomyces cerevisiae* cell wall, *Genetics*, **192** (2012), no. 3, pp. 775-818.

13. De Nobel, J.G.; et al.: The glucanase-soluble mannoproteins limit cell wall porosity in *Saccharomyces cerevisiae*, *Yeast*, **6** (1990), no. 6, pp. 491-499.
14. Guo, B.; et al.: A *Saccharomyces* gene family involved in invasive growth, cell-cell adhesion, and mating, *Proceedings of the National Academy of Sciences*, **97** (2000), no. 22, pp. 12158-12163.
15. Rodríguez-Peña, J.M.; et al.: A Novel Family of Cell Wall-Related Proteins Regulated Differently during the Yeast Life Cycle, *Molecular and Cellular Biology*, **20** (2000), no. 9, pp. 3245-3255.
16. Kogan, G.; et al.: Yeast cell wall polysaccharides as antioxidants and antimutagens: Can they fight cancer? *Minireview*, **55** (2008), no. 5, pp. 387-93.
17. Manners, D.J.; Masson, A.J. and Patterson, J.C.: The structure of a β -(1 \rightarrow 3)-d-glucan from yeast cell walls, *Biochemical Journal*, **135** (1973), no. 1, pp. 19-30.
18. Holan, Z.; et al.: The glucan-chitin complex in *Saccharomyces cerevisiae*, *Archives of Microbiology*, **130** (1981), no. 4, pp. 312-318.
19. Cabib, E.; et al.: The Yeast Cell Wall and Septum as Paradigms of Cell Growth and Morphogenesis, *Journal of Biological Chemistry*, **276** (2001), no. 23, pp. 19679-19682.
20. Geoghegan, I.; Steinberg, G. and Gurr, S.: The Role of the Fungal Cell Wall in the Infection of Plants. **25** (2017), no 12, pp. 957-967.
21. Dwivedi, B.K. and Gibson, D.L.: Processing of Spent Brewers' Yeast for Food Use, *Canadian Institute of Food Technology Journal*, **3** (1970), no. 3, pp. 110-112.
22. Nand, K.: Debitting of spent brewer's yeast for food purposes, *Food/Nahrung*, **31** (1987), no. 2, pp. 127-131.
23. Caballero, I.; Blanco, C.A. and Porras, M.: Iso- α -acids, bitterness and loss of beer quality during storage, *Trends in Food Science & Technology*, **26** (2012), no. 1, pp. 21-30.
24. Bishop, J.R.P.; Nelson, G. and Lamb, J.: Microencapsulation in yeast cells, *Journal of Microencapsulation*, **15** (1998), no. 6, pp. 761-773.
25. Han, L.; et al.: Encapsulation of *Lactobacillus acidophilus* in yeast cell walls (*Saccharomyces cerevisiae*) for improving survival in gastrointestinal conditions, *Journal of Science and Technology*, 2016. p. 54.
26. Dardelle, G.; et al.: Flavour-encapsulation and flavour-release performances of a commercial yeast-based delivery system, *Food Hydrocolloids*, **21** (2007), no. 5, pp. 953-960.
27. Anger, H.M.: *Brautechnische Analysemethoden: Rohstoffe: Gerste, Rohfrucht, Malz, Hopfen und Hopfenprodukte* / hrsg. vom Vorsitzenden Heinz-Michael Anger, 2006: MEBAK.
28. Miedaner, H.: *Brautechnische Analysemethoden, Vol. Band 2*, 2002, Freising-Weihenstephan. X, 332 S.
29. Carneiro, H.C.F.; et al.: Encapsulation efficiency and oxidative stability of flaxseed oil microencapsulated by spray drying using different combinations of wall materials, *Journal of Food Engineering*, **115** (2013), no. 4, pp. 443-451.
30. Pratt, P.L.; Bryce, J.H. and Stewart, G.G.: The Effects of Osmotic Pressure and Ethanol on Yeast Viability and Morphology, *Journal of the Institute of Brewing*, **109** (2003), no. 3, pp. 218-228.
31. Avila-Reyes, S.; et al.: Effect of salt and sugar osmotic stress on the viability and morphology of *Saccharomyces boulardii*, **1** (2016), no. 3, pp. 593-602.
32. Jayanudin, J.; et al.: Microencapsulation Technology of Ginger Oleoresin With Chitosan as Wall Material: A review, *Journal of Applied Pharmaceutical Science*, **6** (2016), no. 12, pp. 209-223.
33. Madene, A.; et al.: Flavour encapsulation and controlled release – a review, *International Journal of Food Science & Technology*, **41** (2006), no. 1, pp. 1-21.
34. Haas, K.; et al.: Impact of powder particle structure on the oxidation stability and color of encapsulated crystalline and emulsified carotenoids in carrot concentrate powders, *Journal of Food Engineering*, **263** (2019), pp. 398-408.
35. Shi, G.; et al.: Chemical treatment and chitosan coating of yeast cells to improve the encapsulation and controlled release of bovine serum albumin, *Artificial Cells, Nanomedicine, and Biotechnology*, **45** (2017), no. 6, pp. 1207-1215.
36. Mokhtari, S.; et al.: Descriptive analysis of bacterial profile, physicochemical and sensory characteristics of grape juice containing *Saccharomyces cerevisiae* cell wall-coated probiotic microcapsules during storage, *International Journal of Food Science & Technology*, **52** (2017), no. 4, pp. 1042-1048.
37. Bringas-Lantigua, M.; et al.: Influence of Spray-Dryer Air Temperatures on Encapsulated Mandarin Oil, *Drying Technology*, **29** (2011), no. 5, pp. 520-526.
38. Tonon, R.V.; Grosso, C.R.F. and Hubinger, M.D.: Influence of emulsion composition and inlet air temperature on the microencapsulation of flaxseed oil by spray drying, *Food Research International*, **44** (2011), no. 1, pp. 282-289.
39. Liu, Y.; et al.: Comparison of the Effects of Different Food-Grade Emulsifiers on the Properties and Stability of a Casein-Maltodextrin-Soybean Oil Compound Emulsion, *Molecules (Basel, Switzerland)*, **25** (2020), no. 3, p. 458.
40. Lindner, M.; Bäuml, M. and Stäbler, A.: Inter-Correlation among the Hydrophilic-Lipophilic Balance, Surfactant System, Viscosity, Particle Size, and Stability of Candelilla Wax-Based Dispersions, *Coatings*, **8** (2018), no. 12, p. 469.
41. Salari, R.; et al.: Characterization of Encapsulated Berberine in Yeast Cells of *Saccharomyces cerevisiae*, *Iranian journal of pharmaceutical research: IJPR*, **14** (2015), no. 4, pp. 1247-1256.
42. Paramera, E.I.; Konteles, S.J. and Karathanos, V.T.: Microencapsulation of curcumin in cells of *Saccharomyces cerevisiae*, *Food Chemistry*, **125** (2011), no. 3, pp. 892-902.

Received 4 May 2020, accepted 5 June 2020